

RhoA/ROCK and Cdc42 Regulate Cell-Cell Contact and N-Cadherin Protein Level during Neurodetermination of P19 Embryonal Stem Cells

Isabel Laplante,^{1,2} Richard Béliveau,² Joanne Paquin¹

¹ Laboratory of Developmental Neuroendocrinology, Département de chimie et biochimie, Université du Québec à Montréal, C.P. 8888, Succ. Centre-ville, Montreal, Quebec, Canada H3C 3P8

² Laboratory of Molecular Medecine, Département de chimie et biochimie, Université du Québec à Montréal, C.P. 8888, Succ. Centre-ville, Montreal, Quebec, Canada H3C 3P8

Received 29 September 2003; accepted 9 January 2004

ABSTRACT: RhoGTPases regulate actin-based signaling cascades and cellular contacts. In neurogenesis, their action modulates cell migration, neuritogenesis, and synaptogenesis. Murine P19 embryonal stem cells differentiate to neurons upon aggregation in the presence of retinoic acid, and we previously showed that RhoA and Cdc42 RhoGTPases are sequentially up-regulated during neuroinduction, suggesting a role at this very early developmental stage. In this work, incubation of differentiating P19 cells with C3 toxin resulted in decreased aggregate cohesion and cadherin protein level. In contrast, C3 effects were not observed in cells overexpressing recombinant dominant active RhoA. On the other hand, C3 did not affect cadherin in uninduced cells and their postmitotic neuronal derivatives, respectively expressing E- and N-cadherin. RhoA is thus influential on cell aggregation and cadherin expression during a sensitive time window that corresponds to the switch of E- to N-cadherin. Cell treat-

ment with Y27632 inhibitor of Rho-associated-kinase ROCK, or advanced overexpression of Cdc42 by gene transfer of a constitutively active form of the protein reproduced C3 effects. RhoA-antisense RNA also reduced cadherin level and the size of cell aggregates, and increased the generation of fibroblast-like cells relative to neurons following neuroinduction. Colchicin, a microtubule disrupter, but not cytochalasin B actin poison, importantly decreased cadherin in neurodifferentiating cells. Overall, our results indicate that the RhoA/ROCK pathway regulates cadherin protein level and cell-cell interactions during neurodetermination, with an impact on the efficiency of the process. The effect on cadherin seems to involve microtubules. The importance of correct timing of RhoA and Cdc42 functional expression in neurogenesis is also raised.

© 2004 Wiley Periodicals, Inc. *J Neurobiol* 60: 289–307, 2004

Keywords: retinoic acid; cell aggregation; C3 toxin; antisense RNA; microtubules

INTRODUCTION

RhoA, Cdc42, and Rac1, the most studied members of the RhoGTPase family, influence the organization of

the actin cytoskeleton. They are viewed as intracellular switches in actin-based transduction cascades that connect environmental signals to the cell nucleus and gene expression (Denhardt, 1996; Hall, 1998; Takai et al., 2001).

Environmental signals can arise from cell-cell contacts that depend on transmembrane proteins such as cadherins. These adhesion proteins are critical to the formation and maintenance of tissue structures. The classical cadherins, such as epithelial cadherin (E-cadherin) and neural cadherin (N-cadherin), have an

Correspondence to: J. Paquin (paquin.joanne@uqam.ca)
Contract grant sponsor: Fondation Charles Bruneau of Hôpital Ste-Justine (Montreal, Quebec, Canada) (R.B.).

© 2004 Wiley Periodicals, Inc.
Published online 1 June 2004 in Wiley InterScience (www.interscience.wiley.com).
DOI 10.1002/neu.20036

extracellular domain that mediates calcium-dependent homophilic interactions and a cytoplasmic tail physically tethered to the actin cytoskeleton as complexes with β/γ -catenin and α -catenin (Yagi and Takeichi, 2000; Fukata and Kaibuchi, 2001). Rho activity is required for the generation and stabilization of E-cadherin-mediated junctions in epithelial and fibroblastic cells (Braga, 2002; Braga et al., 1999, 2000; Takaishi et al., 1997). It is believed that Cdc42 and Rac1 regulate the recruitment of cadherin molecules at the plasma membrane whereas RhoA is thought to act on the actin cytoskeleton distally from the cell surface (Fukata and Kaibuchi, 2001). The GTPase activating proteins IQGAP-1,2 and p190RhoGAP have been identified respectively as partners of Cdc42/Rac1 and RhoA in E-cadherin-mediated cell-cell adhesion (Kaibuchi et al., 1999; Fukata and Kaibuchi, 2001; Natale and Watson, 2002; Noren et al., 2003).

During embryogenesis, stem cells proliferate, form close associations that trigger differentiation, and migrate to their definitive sites where they settle and complete their differentiation program. Several lines of evidence point to the importance of Rho proteins and cadherins in early mammalian development. In mouse, abolition of Rac1 expression perturbed cell adhesion and migration during gastrulation, and Rho inactivation or microinjection of active Cdc42 in blastomeres caused aberrant cell polarization and E-cadherin distribution at cell edges (Sugihara et al., 1998; Clayton et al., 1999). These effects could interfere in the establishment of the axis of polarity in the embryo, a fundamental process for the development of all organisms (Clayton et al., 1999; Redies, 2000). Rho proteins are also involved in late steps of neurogenesis, including neurite extension, cell polarization, and synaptogenesis (Hatten, 1999; Luo, 2000; Laplante et al., 2001; Nikolic, 2002). The RhoA effector p160 Rho-associated kinase ROCK (Rho-associated coiled coil-forming protein kinase) was shown to have a critical role in determining axon outgrowth in CNS neurons (Bitto et al., 2000). On the other hand, cadherin also has a determinant role in neurogenesis as N-cadherin inactivation decreases the number or length of neurites, impairs the formation of neurite growth cones, and engenders defects in neural tissue (Redies, 2000). To what extent N-cadherin and Rho proteins cross-talk during neurogenesis is not known.

Murine P19 cells provide a well established cell differentiation model. They give rise to the formation of cell derivatives of all three germ layers and differentiate using the same mechanisms as normal embryonic stem cells (McBurney, 1993; Jeannotte et al., 1997; Laplante et al., 2001). When cultured into ag-

gregates in the presence of retinoic acid (RA), P19 cells differentiate to neurons (McBurney, 1993; Jeannotte et al., 1997; Cadet and Paquin, 2000). We previously showed that RhoA and Cdc42 are sequentially up-regulated in RA-treated aggregates (Laplante et al., 2001), and Gao et al. (2001) reported a switch from E- to N-cadherin within the first 24 h of treatment, suggesting a role for Rho and N-cadherin in neurodetermination. For cadherin, this hypothesis was supported by the observation that P19 cells overexpressing N-cadherin underwent neurodifferentiation in response to aggregation without the requirement for RA (Gao et al., 2001). In the present work, inactivation strategies were used to determine whether RhoA and its effector ROCK regulate aggregate cohesion and cadherin expression during neuroinduction, and hence influence neurodifferentiation efficiency. Moreover, effect of premature overexpression of Cdc42 was also investigated.

MATERIALS AND METHODS

Preparation of C3 Toxin

The *E. coli* strain BL21 expressing recombinant C3 exoenzyme linked to glutathion-transferase (GST) was described previously (Gingras et al., 2000). Log phase recombinant bacteria were incubated at 32°C with 0.1 mM isopropyl β -D-thiogalactopyranoside (Sigma-Aldrich Canada Ltd., Oakville, Ontario, Canada) until optical density at 540 nm reached 1 unit. Bacteria were centrifuged, resuspended in phosphate-buffered saline (PBS), and lysed by sonication in the presence of protease inhibitors (cocktail inhibitor set I; Calbiochem, San Diego, CA). The lysate was centrifuged at 12,000 \times g for 10 min at 4°C and the supernatant applied onto a glutathion (GSH)-Sepharose 4B column (Amersham Pharmacia Biotech Inc., Baie d'Urfé, Quebec, Canada). After washing the column with PBS, the C3 portion of adsorbed GST-C3 was released by *in situ* cleavage with thrombin (50 U/mL of gel; Amersham Pharmacia Biotech) during 4–6 h. Thrombin eluted with C3 was removed by adsorption onto *p*-amino-benzamidine-agarose (1 μ L agarose beads/mL GSH-Sepharose gel; Sigma-Aldrich). The purity and concentration of C3 preparations were determined by sodium dodecyl sulfate (SDS)-polyacrylamide gel electrophoresis (PAGE) and protein assay, respectively.

Cell Culture, Differentiation, and Treatment

P19 cells were cultured in complete medium containing α -modified Eagle's medium (α -MEM; Gibco-BRL, Burlington, Ontario, Canada) supplemented with 10% heat-inactivated serum (5% donor bovine serum and 5% fetal bovine serum; Cansera International, Rexdale, Ontario,

Canada) and antibiotics (50 U/mL penicillin and 50 $\mu\text{g}/\text{mL}$ streptomycin; Sigma-Aldrich). Cultures were maintained at 37°C, in a 5% CO₂ humidified atmosphere. Neuronal differentiation was done according to Rudnicki and McBurney (1987), with modifications (Laplante et al., 2001). Exponentially dividing P19 cells were seeded at 9×10^4 cells/mL in 35 mm diameter bacteriological-grade dishes (day 0) and grown as aggregates until day 4 in complete medium containing 0.5 μM RA (Sigma-Aldrich). On day 4, aggregates were trypsinized and transferred into gelatinized tissue culture dishes containing serum-free Neurobasal medium supplemented with B27TM supplement and 0.5 mM L-glutamine (Gibco-BRL). Neurobasal medium was prepared by BioMedia Canada Inc. (Drummondville, Quebec, Canada) according to Brewer (1995).

Cells were treated for 24 h by addition of the following agents in the culture media: 30 $\mu\text{g}/\text{mL}$ C3 toxin, 25 μM Y27632 inhibitor (Calbiochem), 5 μM cytochalasin B (Sigma-Aldrich), or 1 μM colchicin (Sigma-Aldrich). Cell morphology was examined with a Nikon inverted microscope and micrographs were taken with Kodak Technical Pan films. Cells were collected for analysis by Western blotting or reverse transcriptase-polymerase chain reaction (RT-PCR). Cell adhesion to dishes was quantified by staining cells with crystal violet (Sigma-Aldrich). The culture medium was removed along with floating cells and the remaining adherent cells were fixed for 1 h in PBS containing 4% p-formaldehyde. Cells were washed with PBS and incubated for 30 min with 0.1% crystal violet in water. Free dye was removed by washing with PBS, and absorbed dye was extracted with 10% acetic acid in water and quantified spectrophotometrically at 595 nm. Cell viability was assessed fluorimetrically by doubly staining cells with acridine orange and propidium iodide followed by cell counting with an hematocytometer (Laplante et al., 2001).

cDNA Plasmids and Cell Transfection

Plasmids pRK5 coding for myc tagged-L63RhoA, -L61Cdc42, and -L61Rac1 were kindly given by Drs A. Hall (University College London, London, UK) and I. Royal (Université de Montréal, Montreal, Quebec, Canada). L63RhoA, L61Cdc42, and L61Rac1, the respective constitutively active forms of RhoA, Cdc42, and Rac1, remained in the GTP-bound state (Ridley, 1997; Royal et al., 2000; Takai et al., 2001). RhoA antisense vector was prepared using the complete cDNA sequence (Adamson et al., 1992). RhoA cDNA was retrieved from pRK5-myc-RhoA vector by digestion with BamHI and EcoRI (Gibco-BRL). After purification by agarose gel electrophoresis and extraction with a QIAquick kit (Quiagen), the RhoA sequence was inserted in the inverse reading orientation by ligation into dephosphorylated pcDNA3.1(-) (Invitrogen Life Technologies, Burlington, Ontario, Canada) predigested with BamHI and EcoRI. Intestine alkaline phosphatase and a Rapid DNA Ligation Kit (Roche Diagnostics, Laval, Quebec, Canada) were used for dephosphorylation and ligation reactions, respectively. The ligated product was amplified

by incorporation into DH5 α competent bacteria prepared as per Chung et al. (1989). Recombinant clones harboring the RhoA antisense insert were identified by screening with Hind III and SmaI (Amersham Pharmacia Biotech), then were propagated and processed with Quiagen MidiPrep kits to purify pcDNA-RhoA antisense.

Transfection of P19 cells with plasmids described above was done using LipofectAMINETM (Gibco-BRL) as per manufacturer's instructions. Subconfluent undifferentiated cells were incubated with the lipofection reagent and plasmid (3.3 μg DNA/60 mm diameter dish) for 5 h in serum-free α -MEM medium supplemented with 10 $\mu\text{g}/\text{mL}$ bovine serum albumin (BSA), 5 $\mu\text{g}/\text{mL}$ transferrin, 1 $\mu\text{g}/\text{mL}$ insulin, and 1 $\mu\text{g}/\text{mL}$ fibronectin (all from Sigma-Aldrich). After removal of this medium, cells were rinsed, cultured for 18 h in complete α -MEM medium, trypsinized, and subjected to neuronal differentiation (aggregation + RA). Mock transfections were done with pRK5 (BD Biosciences, Mississauga, Ontario, Canada) and pcDNA3.1(-) empty vectors. Stable recombinant cells following transfection with pcDNA-RhoA antisense and the corresponding pcDNA3.1(-) empty plasmid were selected over 2 weeks by treatment with 0.4 mg/mL G-418 (Gibco-BRL). At the end of selection clones were subjected to neuronal differentiation in absence of G-418.

Cell Protein Extraction, SDS-PAGE, and Western Blotting

Cells were washed with PBS and extracted by lysis in RIPA buffer (150 mM NaCl, 50 mM Tris, pH 7.6, 1% Nonidet P-40, 0.5% deoxycholate, 0.1% SDS) containing protease inhibitors (Calbiochem's cocktail inhibitor set I). Cell protein extracts (postnuclear extracts) were obtained by centrifugation at 10,000 $\times g$ for 10 min, and resolved (20 μg samples) by SDS-PAGE (Laemmli, 1970) on six 7.5% (cadherin) or 12.5% (Rho GTPases) polyacrylamide gels. Electrotransfer on polyvinylidene difluoride membranes, immunoblotting, chemiluminescent immunodetection, and densitometric analysis of autoluminograms were done as described (Laplante et al., 2001). Primary antibodies were used at the indicated dilutions: mouse monoclonal anti-RhoA, rabbit polyclonal anti-Cdc42, and rabbit polyclonal anti-RhoB (all from Santa Cruz Biotechnology, Santa Cruz, CA), 1/500; mouse monoclonal anti-myc (Santa-Cruz), 1/500; mouse monoclonal anti-Rac1 (BD Biosciences), 1/4000; mouse monoclonal anti-pan-cadherin recognizing all cadherin isoforms (Sigma-Aldrich), 1/1000; rabbit anti-extracellular signal-regulated kinase (Erk; Cell Signaling Technology, Beverly, CA), 1/500; and rabbit polyclonal anti-neurofilament-M (Chemicon International Inc., Temecula, CA), 1/1000.

Protein Assay

Protein content was evaluated by the Bradford dye binding assay (Bio-Rad, Mississauga, Ontario, Canada), or, for detergent-containing samples, by a micro-BCA assay using a

Table 1 Time Courses of Several P19 Cell Differentiation Protocols

Determination Period Days 0–4	Maturation Period Day 4 and After	Resulting Phenotype Days 6–8
Aggregates + 0.5 μ M RA	Monolayers	Neurons (>95%)
Monolayers + 0.5 μ M RA	Monolayers	Fibroblast-like cells (>80%)
Aggregates + no inducer	Monolayers	Undifferentiated (>90%)
Monolayers + no inducer	Monolayers	Undifferentiated (>95%)

Differentiation protocols are carried out over 6–8 days. Aggregates are obtained by culturing cells in bacteriological grade dishes while tissue grade dishes are used for monolayers. Neurons, fibroblast-like cells, and undifferentiated cells are identifiable morphologically and immunologically (Rudnicki and McBurney, 1987; Jeannotte et al., 1997; Cadet and Paquin, 2000; Laplante et al., 2001). Numbers in parentheses indicate the percentages of cells exhibiting the indicated phenotypes.

kit from Pierce Chemical Co. (Rockford, IL). BSA was used as the standard with both assays.

RT-PCR

Total RNA was extracted from P19 cells using Trizol reagent (Gibco-BRL) according to the manufacturer's instructions. cDNAs were synthesized from 5 μ g of total RNA at 50°C for 30 min using a Superscript RT/Platinum Taq kit (Gibco-BRL) and amplified by PCR in a Gene-AMP PCR system 9700 (Perkin-Elmer, Wellesley, MA). The E- and N-cadherin specific sense and antisense 20-oligonucleotide primers (Sheldon Biotechnology Centre, Montreal, Quebec, Canada) were derived from murine sequences (Gao et al., 2001). Amplifications started with 0.2 μ M primers and 200 μ M dNTP, and were performed over 25 cycles, each involving 45 s at 94°C, 45 s at 57°C, and 1.5 min at 72°C. Glyceraldehyde-3-phosphate dehydrogenase (GAPDH) primers and amplification conditions were as described elsewhere (Paquin et al., 2002). RT-PCR products were analyzed on 1.2% agarose gels containing 0.4 μ g/mL ethidium bromide.

Statistics

Statistical analysis was done using Student's *t* test. Unless otherwise indicated, $p < 0.05$ was used as the significance level.

RESULTS

RhoA Influences Cellular Contacts and Cadherin Protein Level during Neurodetermination

As depicted in Table 1, neuronal differentiation of P19 cells requires both cell aggregation and the presence of RA during the determination period. Treatment with RA applied to cell monolayers induces differentiation to fibroblast-like cells, and absence of the inducing agent leaves most cells in their undifferentiated state. To test the possibility that RhoA influ-

ences cell aggregation and cadherin expression during neuronal differentiation, we first inactivated Rho by treating cells with C3 toxin, an exoenzyme that ADP-ribosylates RhoA, RhoB, and RhoC (Kjøller and Hall, 1999).

Under normal culture conditions, undifferentiated P19 cells adhere to, and flatten on, the surface of tissue culture dishes [Fig. 1(a), photo 1]. However, they associate into floating compact aggregates in bacteriological-grade dishes in the presence of RA, and aggregate size increases with time [Fig. 1(a), photos 2 and 3]. Exposure to 30 μ g/mL C3 for 24 h affected cell morphology. Undifferentiated cells took a spindle-like shape while remaining attached to the tissue-grade surface by cytoplasmic stretches [Fig. 1(a), photo 5]. Similar C3-induced morphological changes were shown to correlate with destruction of actin stress fibers in adherent glial and neuronal cell cultures (Barth et al., 1999; Lehman et al., 1999). When C3 treatment was applied at day 0 of aggregation in the presence of RA, almost no aggregate formed and an important proportion of the cells attached to bacteriological-grade surfaces that normally do not allow cell adhesion [Fig. 1(a), photo 6]. C3-induced cell adhesion to the culture support was concentration-dependent, as assayed by staining with crystal violet, and reached a maximum between 20 and 50 μ g/mL of the toxin [Fig. 1(b)]. For this reason, the concentration of 30 μ g/mL C3 was adopted throughout. Addition of C3 at day 1 of differentiation when aggregates were already formed decreased aggregate cohesion [Fig. 1(a), photo 7]. Aggregates had irregular contours due to loosely bound cells at their surface and numerous small aggregates were seen that could represent pieces released from larger aggregates. Aggregates were also found to be easily disruptable by pipetting, another sign of decreased cohesiveness, and a number of them adhered to the bacteriological-grade surfaces. Morphological changes in RA-treated aggregates were not due to viability loss

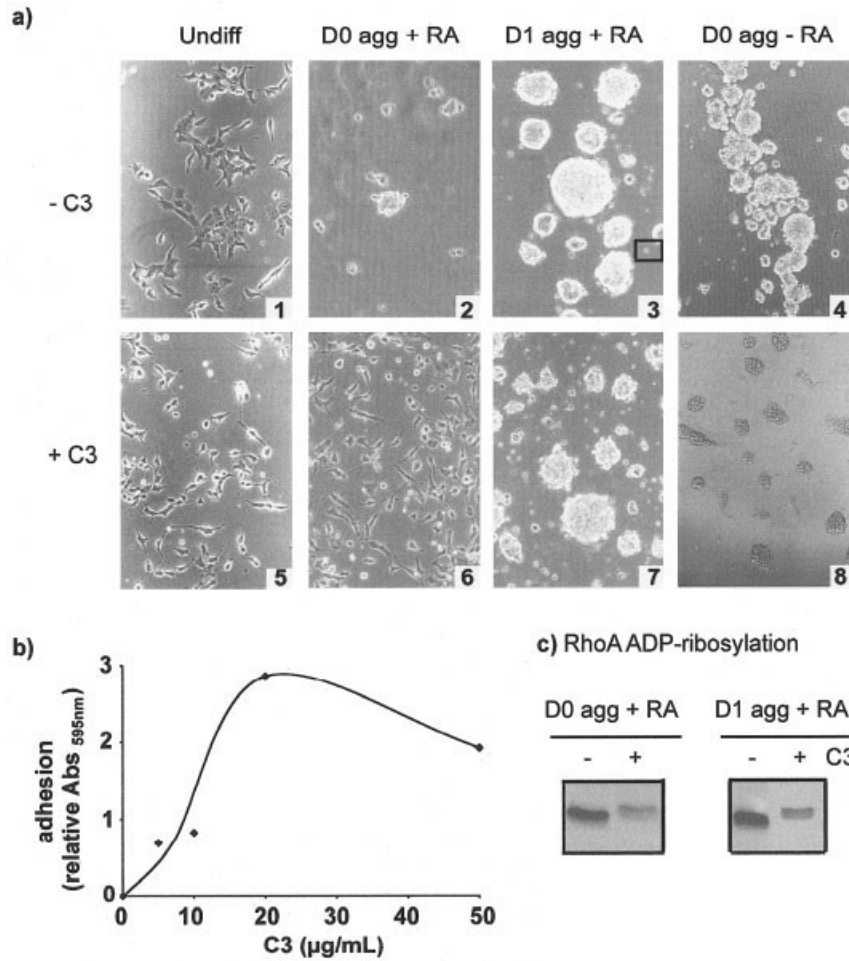


Figure 1 C3 impairs cell aggregation during neurodetermination. (a) P19 cells were treated with 30 μg/mL C3 toxin for 24 h in their undifferentiated state (undiff), or starting at day 0 (D0) or day 1 (D1) of the neurodifferentiation protocol. For comparison, D0 aggregates not exposed to differentiating conditions (-RA) were also studied. Micrographs were taken at 200X magnification at the end of treatment and are representative of at least three independent experiments. The square contains a single cell for size reference. (b) P19 cells were incubated with different concentrations of C3 toxin for 24 h at D0 of neurodifferentiation. Cell adhesion to bacteriological-grade dishes was assayed spectrophotometrically after staining with crystal violet. (c) ADP-ribosylation was evaluated by SDS-PAGE (20 μg cell lysate proteins per lane) followed by RhoA immunoblotting.

because no significant mortality was observed for C3 concentrations up to 50 μg/mL (not shown). Rather they resulted from Rho ADP-ribosylation because the RhoA immunoreactive band completely shifted towards higher Mr by SDS-PAGE [Fig. 1(c)], as expected (Barth et al., 1999; Beltman et al., 1999). The reduced intensity of the RhoA immunoreactive signal following C3 treatment was due to the decreased affinity of the antibody for ADP-ribosylated RhoA as compared to the unmodified protein (Beltman et al., 1999; Lehmann et al., 1999). Thus, during RA-induced neurogenesis, C3 impaired cell-cell contact as revealed by loss of aggregate cohesion. Interestingly,

day 0 aggregates not induced with RA appeared more resistant to disaggregation during C3 treatment. Under these conditions, cells adsorbed as clumps on bacteriological-grade surfaces [Fig. 1(a), photos 4 and 8], although adsorption was weak. C3 thus exhibited a disaggregating effect only in the presence of RA.

To appreciate the effect of Rho inactivation on cadherin level, we first determined the influence of RA and aggregation on cadherin expression profiles. Figure 2(a) (lane 1) shows that N- and E-cadherin transcripts were present in undifferentiated cells, as reported previously (Gao et al., 2001). E-cadherin

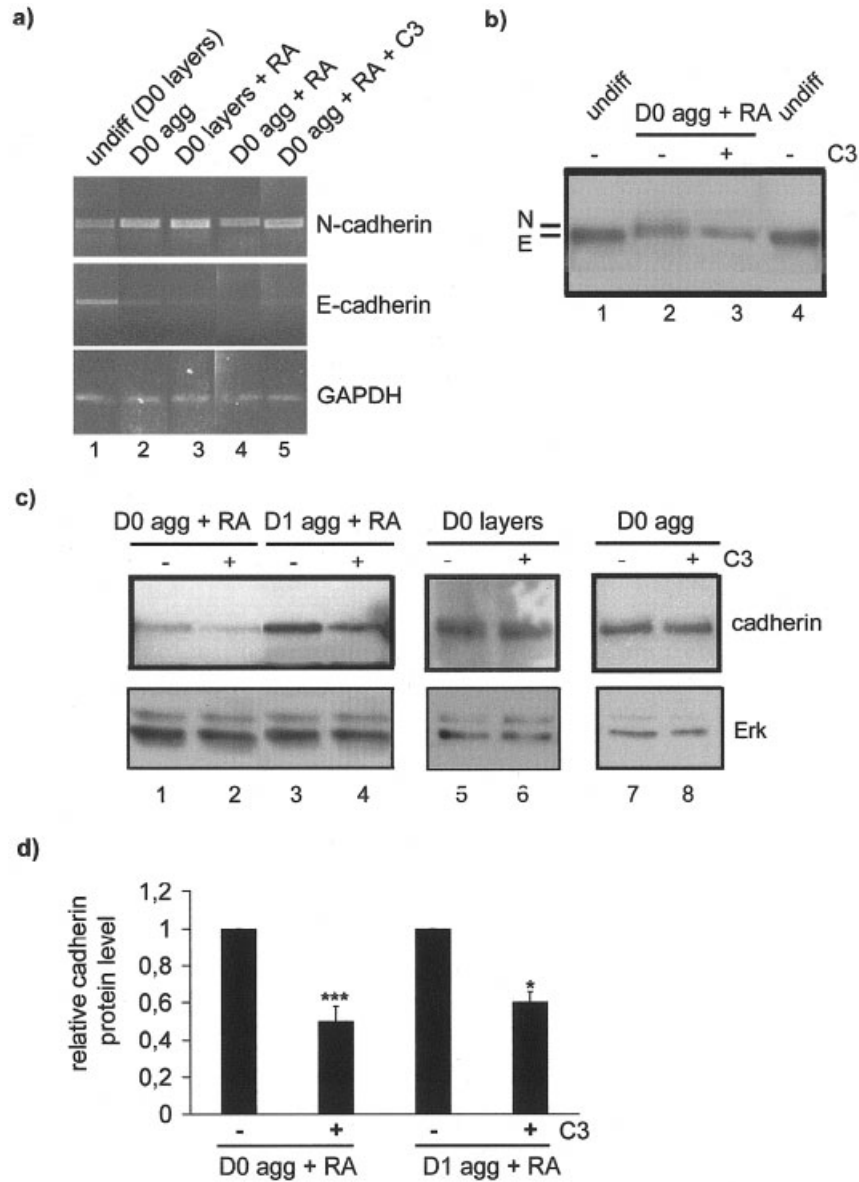


Figure 2 C3 reduces N-cadherin protein expression during neurodetermination. P19 cells were incubated with or without 30 $\mu\text{g}/\text{mL}$ C3 toxin for 24 h at day 0 (D0) or day 1 (D1) of various cell differentiation protocols. (a) RT-PCR for N- and E-cadherin using GAPDH as a control. (b,c) Pan-cadherin immunoblots following SDS-PAGE done in 6% (b) or 7.5% (c) polyacrylamide gels. Erk immunoreactivity served to verify protein loads on gels. (d) Densitometric analysis of cadherin blots obtained in (c) with RA-induced aggregates. Results are expressed as the means \pm SEM, and the symbols * and *** respectively indicate significant ($p < 0.05$) and very highly significant ($p < 0.001$) difference with corresponding C3-untreated cells. All results are representative of three independent studies. Layers, monolayers; agg, aggregates; undiff, undifferentiated (in these experiments, undifferentiated cells refer to uninduced cell monolayers).

transcript levels decreased in uninduced aggregates (lane 2), in RA-induced monolayers (lane 3), and furthermore when RA treatment and aggregation were combined (lane 4). In contrast, N-cadherin transcript was present at similar levels in all of these conditions. Similar to the results of Gao et al. (2001), Western

blotting using pan-cadherin antibody showed that E-cadherin protein was replaced by N-cadherin at the beginning of the neurodifferentiation protocol, as demonstrated by reduction of cadherin electrophoretic mobility [Fig. 2(b), compare lane 2 with lanes 1 and 4]. We did not succeed in discriminating E- and

N-cadherin using a number of commercially available isoform-specific antibodies. The specific antibodies tested were much less sensitive than the pan-cadherin antibody and could not detect the low level of N-cadherin at day 1 of neurodifferentiation. Overall, RT-PCR and differential electrophoresis thus indicated that aggregation and RA turn off E-cadherin expression.

C3-treatment of P19 cells induced with RA + aggregation for 24 h did not inhibit the switch from E- to N-cadherin protein [Fig. 2(b), lanes 2 and 3]. However, application of the treatment at day 0 as well as at day 1 of the neurodifferentiation protocol significantly decreased cadherin protein level by 50% [Fig. 2(c), lanes 1–4, and Fig. 2(d)]. Notice the higher levels of cadherin at day 1 compared to day 0 in absence of C3 [Fig. 2(c), lanes 3 and 1], in agreement with the reported increasing levels of N-cadherin with time during neurodifferentiation (Gao et al., 2001). In contrast to protein expression level, cadherin mRNA level was not significantly affected by C3 [Fig. 2(a), compare lanes 4 and 5 for E- and N-cadherin]. On the other hand, C3 did not decrease cadherin protein level in undifferentiated cells that express the E-isoform [Fig. 2(c), compare lanes 5 and 6, and lanes 7 and 8]. The stability of cadherin expression in undifferentiated cells could explain their resistance to C3-induced disaggregation [Fig. 1(a), photo 8]. C3 thus has an effect on N-cadherin protein level at the beginning of the neurodifferentiation protocol.

Because RhoA is not the sole target of C3 and moreover it can exist as a GDP-bound inactive form in addition to a GTP-bound active form, its implication in cadherin regulation was confirmed by overexpressing constitutively active RhoA (L63RhoA) in cells. Undifferentiated P19 cells were transiently transfected with myc tagged-L63RhoA or empty vector (pRK5) [Fig. 3(a)], and subjected to neuronal differentiation in the absence or presence of C3. There was no significant difference in the size of aggregates between both cell populations. Mock-transfected cells responded like wild-type cells to C3 treatment. Cell aggregation was reduced (and accompanied by adhesion to bacteriological-grade surfaces) [Fig. 3(b)] and cadherin protein level significantly decreased by 50% [Fig. 3(c,d)]. In contrast, C3 had no significant effect on culture morphology [Fig. 3(b)] and cadherin level [Fig. 3(c,d)] in L63RhoA-transfected cells. Overexpression of constitutively active RhoA was thus sufficient to counteract C3 effect on cadherin.

That C3 had no influence on E-cadherin level while it reduced N-cadherin at neurodetermination could be due to an isoform- and/or stage-specific effect. We investigated these possibilities by analyz-

ing toxin effect on cadherin level at day 4 of the neurodifferentiation program. At this stage, cells are postmitotic neurons expressing high levels of N-cadherin but no E-cadherin (Gao et al., 2001). Twenty-four hours after their transfer from bacteriological- to tissue-grade dishes, newly generated neurons had adhered to the culture surface and started to grow neuritic extensions [Fig. 4(a), photo 2], as we previously reported (Laplante et al., 2001). C3 treatment induced P19 neurons to adopt a spindle-like shape [Fig. 4(a), photo 4], as reported for other neuronal cell models (Jalink et al., 1994; Hirose et al., 1998). When day 4 cells were put back in bacteriological dishes after trypsinization, they reformed aggregates [Fig. 4(a), photo 1]. C3 treatment prevented reaggregation while stimulating cell adhesion to the surface [Fig. 4(a), photo 3]. C3-induced morphological effects were associated with Rho ADP-ribosylation [Fig. 4(c)]. RhoA was completely ADP-ribosylated by the toxin as well as RhoB, which is up-regulated at this time of neurodifferentiation (Laplante et al., 2001). Cdc42 was not modified by C3, as expected, due the lack of Asn⁴¹ (Kjøller and Hall, 1999). Despite the efficiency of ADP-ribosylation and morphological changes induced by C3 in postmitotic neurons, the toxin had no significant effect ($p > 0.05$) on cadherin protein level [Fig. 4(b)], indicating a “time window”-dependent susceptibility of cadherin to Rho inactivation during neurodifferentiation. The susceptibility period is at neurodetermination, contemporaneously to the E- to N-cadherin switch.

RhoA Antisense cDNA Decreases Cadherin Expression and Neurodifferentiation Efficiency

Under our culture conditions, the neurodifferentiation protocol generates cell populations containing as much as 95% neurons at day 7, the remainders being fibroblast-like cells (Table 1). We wanted to inactivate RhoA over the entire 7 day period in order to evaluate consequences on neurodifferentiation efficiency. C3 treatment could not be used for more than 24 h because cell death occurred. In addition, C3 was not specific to RhoA. We thus transferred the cDNA of constitutively inactive RhoA (myc tagged-N19RhoA; Sebök et al., 1999), but abandoned this strategy because of very low expression in recombinant cell populations ($\leq 10\%$ of endogenous RhoA levels). We turned to antisense inactivation strategy and produced stable P19 recombinants for RhoA antisense as well as for empty pcDNA3.1(-) plasmid as a control. Twenty-four clones of each population were picked out and expanded. Of these, eight to nine cell

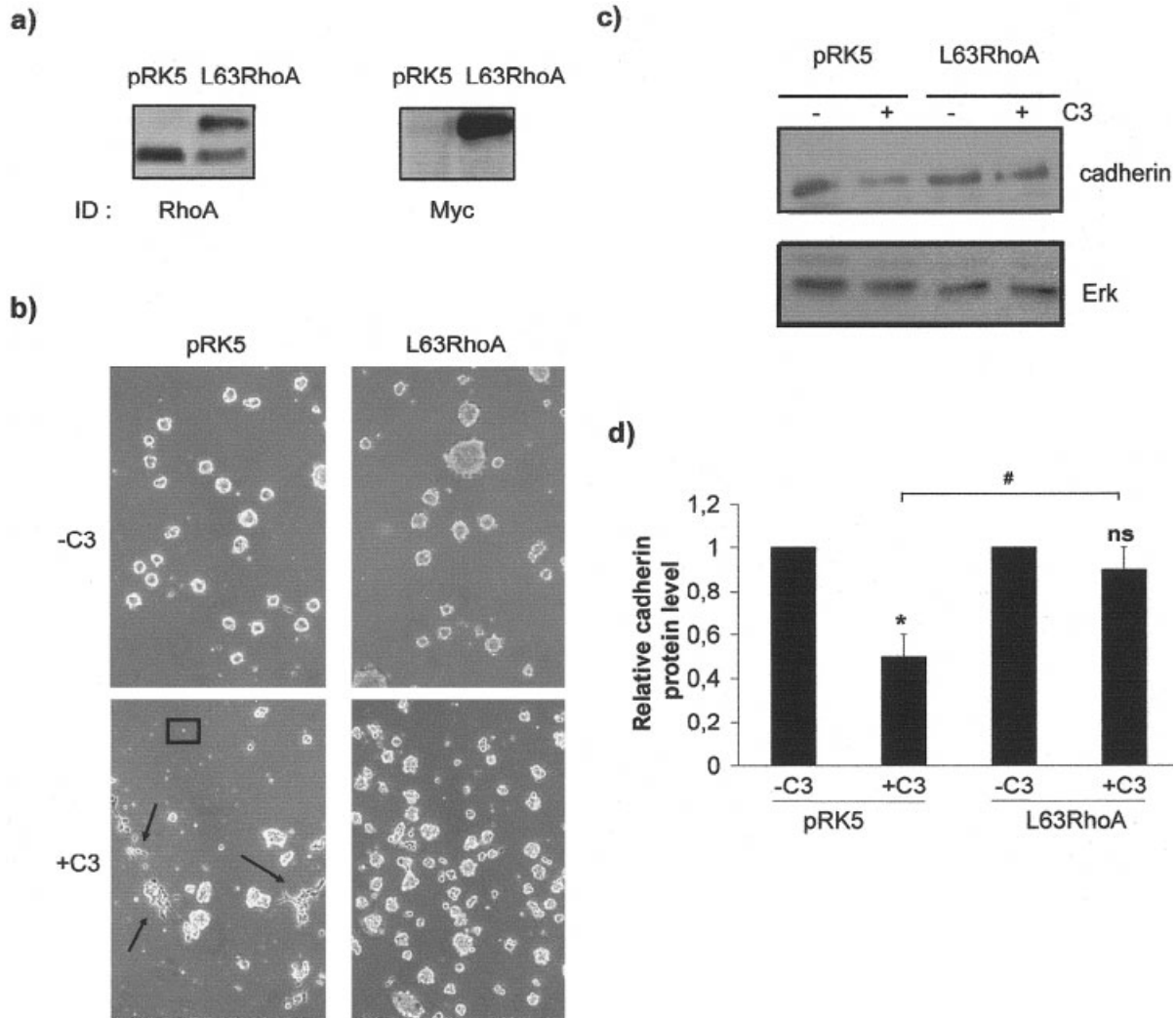


Figure 3 Overexpression of active RhoA prevents C3 effects during neurodetermination. P19 cells were transiently transfected with myc tagged-L63RhoA cDNA or empty pRK5 plasmid (control), and subjected to the first day of the neurodifferentiation protocol in the absence or presence of 30 $\mu\text{g}/\text{mL}$ C3. (a) Immunodetection (ID) of RhoA and myc by Western blotting 24 h post-transfection. (b) Cell morphology after C3 treatment (100X). The square contains a single cell for size reference and arrows point to adhered cells. (c) Pan-cadherin Western blots after C3 treatment, using Erk immunoreactivity as a control for gel loading. (d) Densitometric analysis of pan-cadherin Western blots. Results are expressed as the means \pm SEM of five independent experiments. The symbols * and ns respectively indicate significant and no significant difference with corresponding C3-untreated cells. The symbol # indicates a significant difference between pRK5 +C3 and L63RhoA +C3.

clones were subjected to neuronal differentiation. Because Rho proteins were reported to have a role in cell cycle, the eight to nine clones were selected on the basis that their proliferation rates resembled that of wild-type cells in order to avoid the possibility that differences in aggregate sizes were due to differences in proliferation rates. Most probably because of this criteria, selected RhoA antisense clones had decreased but not abolished RhoA expression.

In the undifferentiated state, antisense clones had similar morphology as control clones (not shown) but only half the protein levels of RhoA and cadherin [Fig. 5(a), Undiff]. RhoA was selectively targeted by the antisense strategy because there was no significant changes in RhoB protein levels despite the strong homology that exists between RhoA and RhoB (85%; Ridley, 1997). The decreased cadherin level in undifferentiated antisense clones was unexpected given the

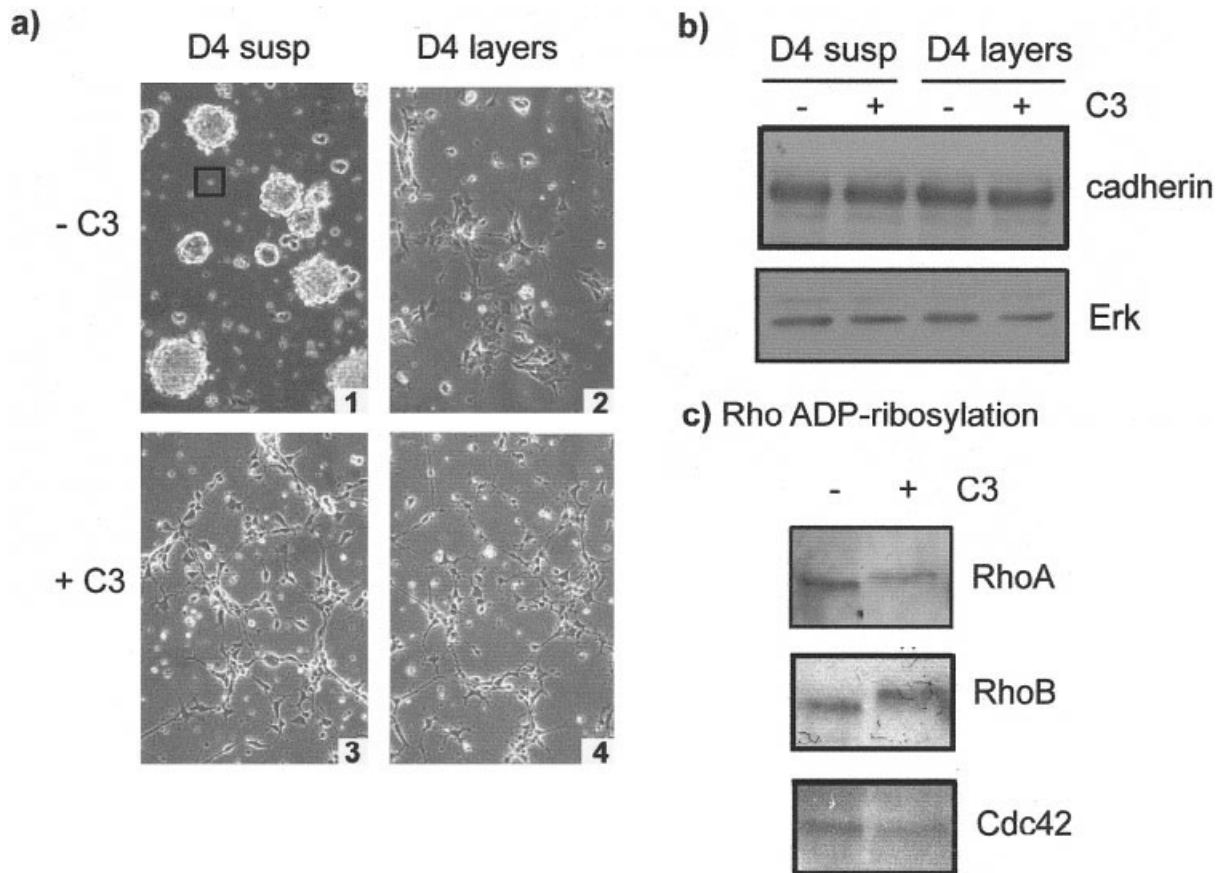


Figure 4 C3 does not reduce cadherin protein expression in postmitotic P19 neurons. P19 cell aggregates were subjected to neurodifferentiation with RA for 4 days in bacteriological-grade dishes. At day 4, cells were trypsinized and cultured in bacteriological-grade dishes (D4 susp) or tissue culture dishes (D4 layers) for 24 h, in the absence or presence of 30 $\mu\text{g}/\text{mL}$ C3. (a) Cell morphology (200X). The square contains a single cell for size reference. (b) Pan-cadherin Western blots, using Erk immunoreactivity as a control for gel loading. (c) ADP-ribosylation was evaluated by SDS-PAGE (20 μg cell lysate proteins per lane) followed by RhoA, RhoB, and Cdc42 immunoblotting. All results are representative of three independent experiments.

lack of C3 effect on cadherin level in wild-type cells [Fig. 2(c)]. The discrepancy could have arisen from a metabolic adaptation of the cells to a situation of long term reduction in RhoA levels in comparison to the punctual reduction associated with C3 treatment. Differences in RhoA and cadherin levels were maintained during the 4 days of aggregation in the presence of RA [Fig. 5(a), Day 2 and Day 4]. The incidence of aggregates of small size or reduced cohesiveness was higher in antisense than control clones (63 vs. 22% of clones). In contrast to what was observed with C3 treatment there was little or no adhesion of antisense cells on bacteriological-grade surfaces, most probably because the antisense construct did not completely abolish RhoA expression/activity as compared to the inactivating action of C3. Almost all clones generated neurons when examined

at day 7 but they differed in the degree of contamination with fibroblast-like cells. Contamination degrees were defined as follows: 5% indicates that few fibroblast-like cells are seen underneath some islets of neurons; 30% indicates that fibroblastic islets are seen underneath most of the neuronal islets; 70% indicates that fibroblast-like cells form a confluent or almost-confluent cell layer over which are found many neuronal islets; and 90% indicates that there remain only rare islets of neurons over the confluent fibroblastic layer. High contamination by fibroblast-like cells ($\geq 30\%$ of the cell culture) appeared more often in antisense than in control populations (82 vs. 28% of clones). One antisense clone had low levels of both RhoA and cadherin ($< 25\%$ of control values) over the entire aggregation period (day 0 to day 4). It had the same culture morphology as wild-type cells in the

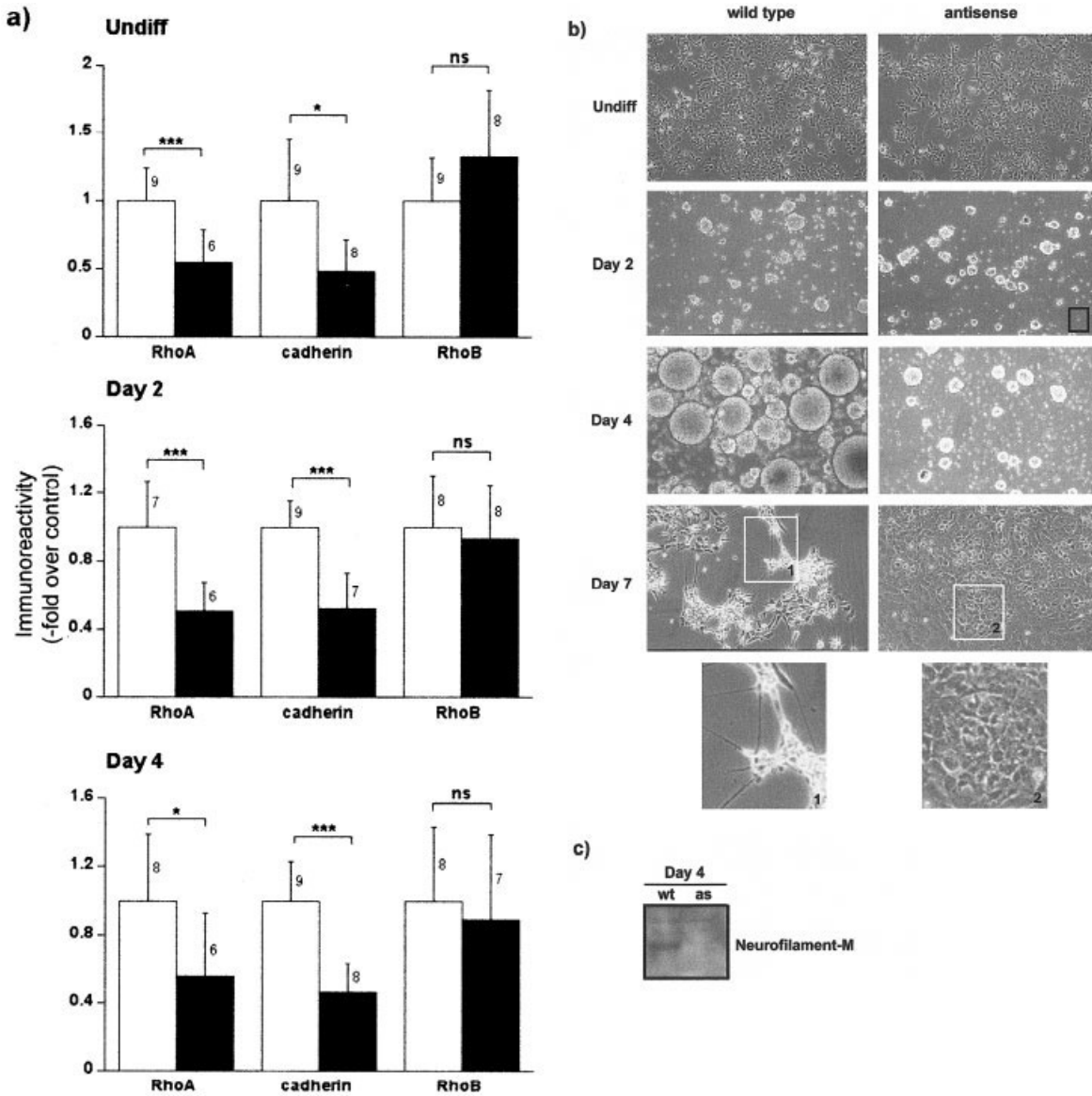


Figure 5 RhoA-antisense cDNA decreases cadherin protein expression and neurodifferentiation efficiency. P19 cells were stably transfected with RhoA antisense cDNA or empty pcDNA3.1(-) plasmid (control). A number of clones (eight to nine for each group) were propagated and subjected to neuronal differentiation. (a) Cells were collected in their undifferentiated state and at days 2 and 4 of neurodifferentiation, and analyzed by Western blotting for RhoA, cadherin, and RhoB. The intensity of immunoreactive signals in antisense clones (filled bars) is expressed relative to control clones (empty bars). Results are reported as the means \pm SD for the number of determinations indicated above each bar. The symbols ns, *, and *** respectively indicate no significant, significant, and very highly significant ($p < 0.001$) differences with controls. (b) Cell morphology in the undifferentiated state and at days 2, 4, and 7 of the neuronal differentiation protocol. Micrographs (100X) are shown for wild-type cells and a RhoA antisense clone having low RhoA and cadherin levels. The black square contains a single cell for size reference during aggregation (days 2 and 4). Cellular fields within a white box in day 7 micrographs are also shown as 2.5-fold enlarged pictures; compare the compact cell bodies and long neuritic processes of neurons (box 1) with the large cytosolic surface of fibroblast-like cells (box 2). (c) Neurofilament-M Western blotting of day 4 cell cultures presented in (b); wt, wild-type; as, antisense.

undifferentiated state but generated only small aggregates at days 0–4 and gave rise to almost exclusively fibroblast-like cells by day 7 instead of neurons [Fig. 5(b)]. The absence or rarity of neurons was confirmed by the absence of neurofilament-M neuronal marker by immunoblotting [Fig. 5(c)]. At day 7 of neurodifferentiation, there was lower N-cadherin protein level in antisense than in wild-type cells (not shown). However, it was not possible to define exactly the contribution of the RhoA antisense construct and the new differentiated phenotype in this reduction of cadherin expression. Indeed fibroblast-like cells generated from RA-induced P19 cell monolayers (Table 1) naturally do express N-cadherin and this, at a lower level than found in P19 neurons (not shown). A second transfection series gave a similar collection of results. RhoA level thus has an influence on aggregation and neurodifferentiation efficiency. In fact, RA treatment in conditions of reduced cell aggregation favored the generation of fibroblast-like cells, as does RA treatment on cell monolayers (Table 1).

Inhibition of ROCK during Neurodetermination Mimics the Effects of C3 Toxin

Among the putative target molecules of Rho, ROCK is believed to be implicated in RhoA-mediated cell adhesion/motility and neurite extension/retraction (Bito et al., 2000; Amano et al., 2000; Takai et al., 2001). We evaluated whether the selective inhibition of this kinase with Y27632 could reproduce the effects of Rho inactivation during neurodetermination of P19 cells. This was found to be the case. Indeed, Y27632 stimulated cell adhesion to bacteriological dishes instead of supporting aggregation [Fig. 6(a), photos 1 and 3] and decreased cohesion of day 1 aggregates [Fig. 6(a), photos 2 and 4]. Figures 6(b) and 6(c) show that these morphological effects were accompanied by reduced cadherin protein level. Day 0 and day 1 inhibited cells had, respectively, 50% ($p < 0.05$) and 30% ($p < 0.001$) the cadherin level of corresponding uninhibited cells. Similar to Rho inactivation by C3, there was no apparent effect on E- or N-cadherin mRNA level [Fig. 6(d)]. Our results thus indicate that the RhoA/ROCK pathway helps in maintaining adequate cell-cell contact and cadherin protein level during neurodetermination.

Premature Overexpression of Active Cdc42 Affects Cellular Contacts and Cadherin Protein Level

RhoA up-regulation is followed by that of Cdc42 in neurally differentiating P19 cells, with Cdc42 expres-

sion becoming maximal when RhoA goes back to basal levels (Laplante et al., 2001). Constitutively active recombinant Cdc42 (myc tagged-L61Cdc42) was expressed in P19 cells to test the impact of advanced up-regulation on aggregation and cadherin. We also overexpressed active Rac1 (myc tagged-L61Rac), a Cdc42 cognate involved in the regulation of cadherin-mediated cell-cell contact (Braga et al., 1999, 2000). At 18 h post-transfection, about 30–50% of P19 cells incorporated the transgenes, and total Cdc42 and Rac levels were, respectively, five- and 10-fold the wild-type values [Fig. 7(a)]. Like wild-type cells, cells transfected with empty plasmid (pRK5) and subjected to neurodifferentiation formed floating aggregates in bacteriological-grade dishes [Fig. 7(b)]. L61Rac1- and L61Cdc42-transfected populations formed aggregates but of smaller sizes and contained numerous adherent cells [Fig. 7(b)]. Adherent cells represented about 20–30% of total populations, likely reflecting individual cell difference in expression level of recombinant proteins. L61Rac- and L61Cdc42-transfected cell cultures also exhibited a decreased cadherin protein level compared to pRK5 cultures [Fig. 7(c,d); –C3]. C3 treatment further amplified cadherin reduction [Fig. 7(c,d); +C3] and cell adhesion to bacteriological surfaces (not shown). Thus, like RhoA inactivation, overexpression of Cdc42 or Rac1 during neurodetermination decreased cadherin protein level and cell-cell interaction.

Effects of Cytoskeleton Disrupters on Cadherin Level during Neurodetermination

RhoGTPases are now well established as modulators of actin cytoskeleton organization while their possible implication in microtubule networking has only begun to emerge (Arthur et al., 2002; Liu et al., 1998; Wittmann and Waterman-Storer, 2001). The stability of cadherin mediated cell-cell junctions requires actin cytoskeleton, but the work of Mary et al. (2002) recently showed that microtubules are necessary for the transport of N-cadherin to the plasma membrane. We therefore used cytoskeleton disrupters to determine whether C3 reducing effect on cadherin level in neurally differentiating P19 cells could be related to the disorganization of actin and/or microtubule networks. Cells were treated during 24 h with 5 μ M cytochalasin B or 1 μ M colchicin, starting at day 0 of the neurodifferentiation protocol. These conditions were shown to affect cytoskeleton but not cell viability (Laplante et al., 2001). In wild-type cells, cytochalasin B, a disrupter of actin filaments, had no significant effect on aggregate cohesion or cadherin protein

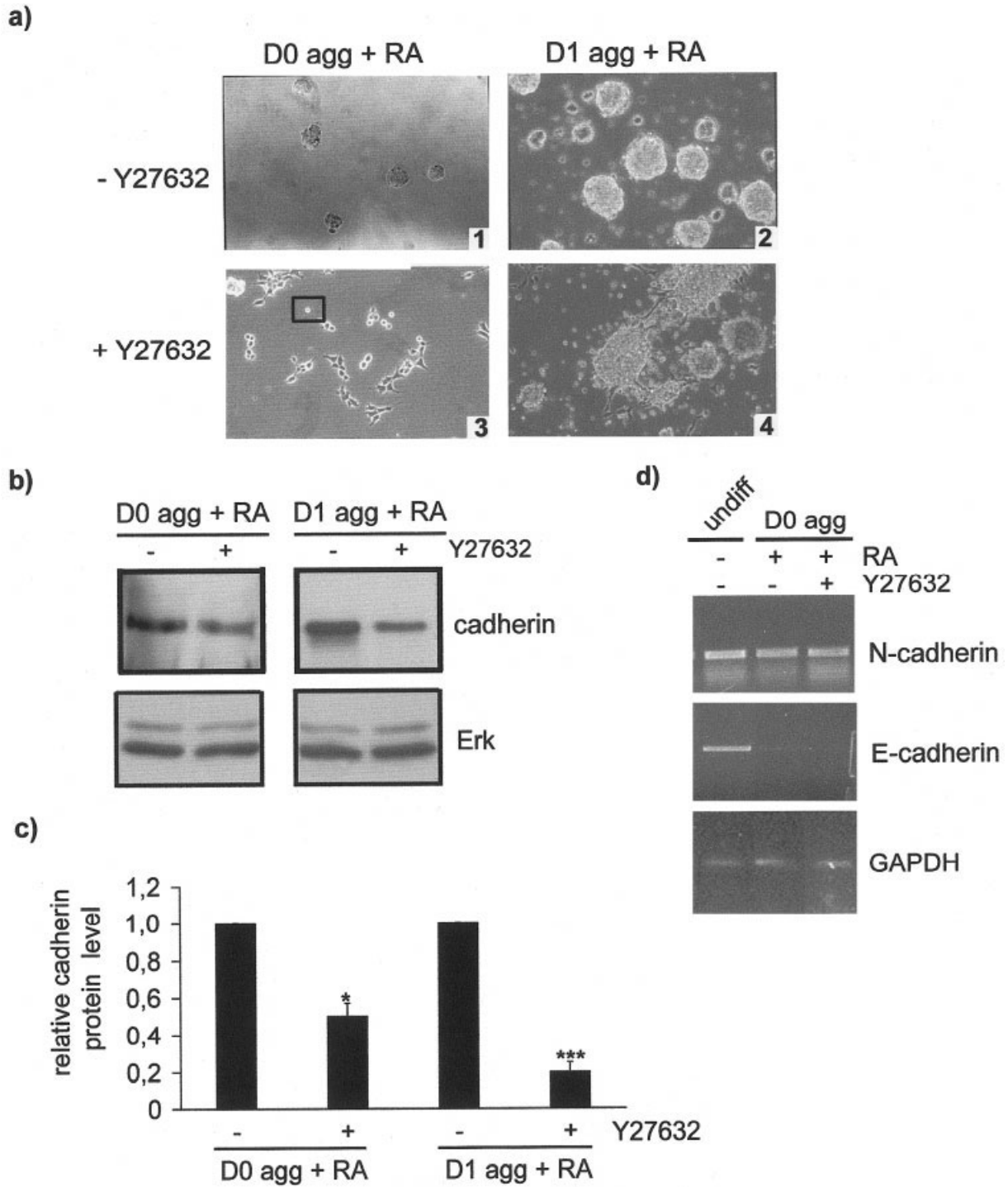


Figure 6 ROCK inactivation reduces cell aggregation and cadherin protein level during neuro-determination. Cells were treated with 25 μ M Y27632 for 24 h, starting at day 0 (D0) or at day 1 (D1) of the neurodifferentiation protocol. (a) Cell morphology (200X). The square contains a single cell for size reference. (b,c) Pan-cadherin Western blotting and densitometric analysis. Results are expressed as the means \pm SEM, and the symbols * and *** respectively indicate significant ($p < 0.05$) and very highly significant ($p < 0.001$) difference with corresponding cells not treated with Y27632. Erk immunoreactivity was used as a control for gel loading. (d) RT-PCR for N- and E-cadherin using GAPDH as a control. All results are representative of three independent experiments.

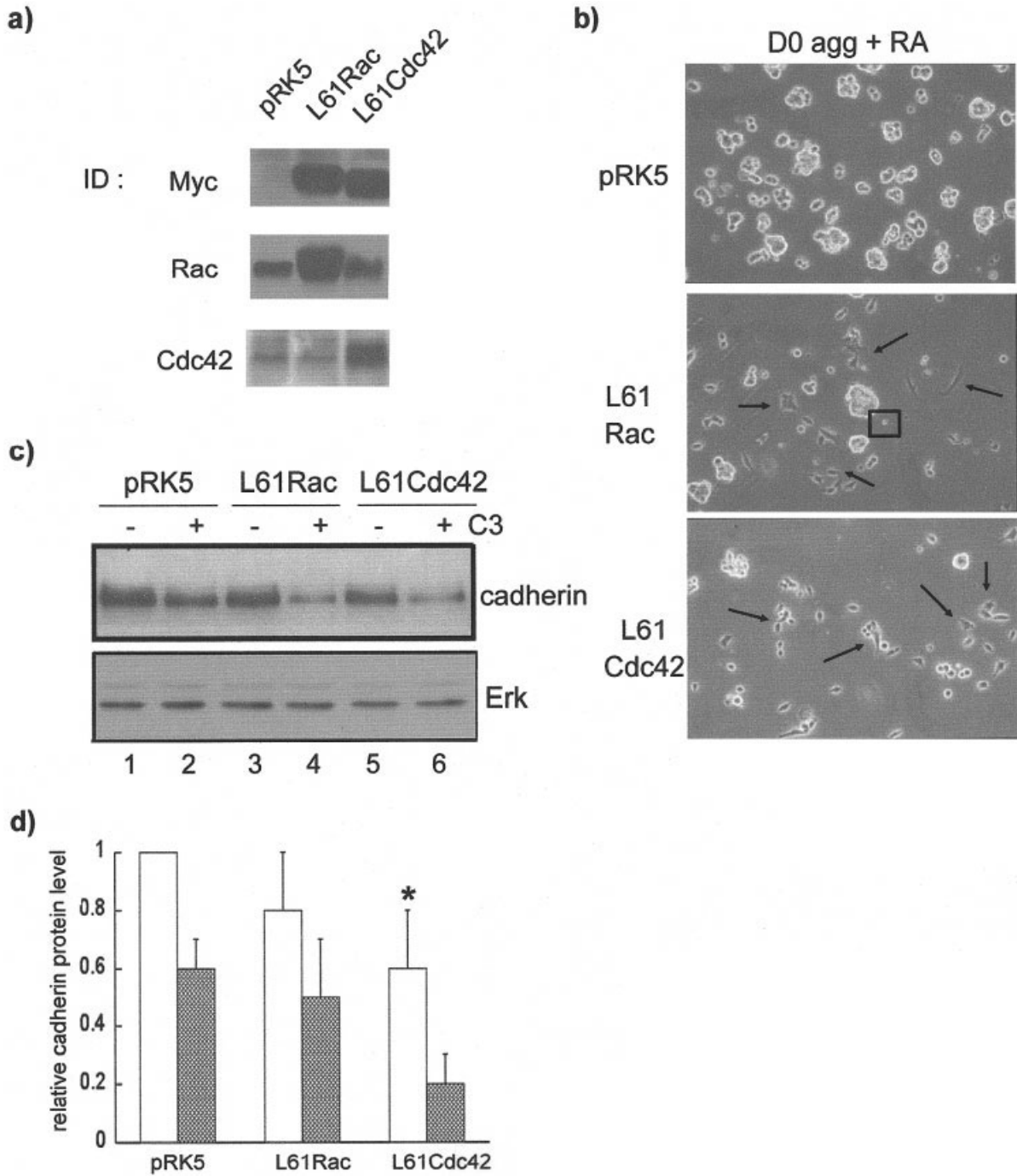


Figure 7 Overexpression of Cdc42 and Rac reduces cell aggregation and cadherin protein level during neurodetermination. P19 cells were transiently transfected with pRK5 empty plasmid (control) or with plasmid carrying a myc tagged-L61Rac1 or -L61Cdc42 cDNA. Cells were then subjected to the first 24 h of the neurodifferentiation protocol in the absence or presence of 30 $\mu\text{g}/\text{mL}$ C3. (a) Immunodetection (ID) using anti-myc, anti-Rac, and anti-Cdc42 antibodies. (b) Cell morphology (200X). Photographs show cells not treated with C3. The square contains a single cell for size reference and arrows point to adhered cells. (c,d) Cadherin immunoblotting comparing transfected cells not treated and treated with C3. Erk immunoreactivity was used as a control for gel loading. Densitometry values are expressed relative to pRK5 cells not treated with C3. Four independent studies were done in the absence of C3 and results are reported as the means \pm SD, with * indicating a significant difference between corresponding pRK5 cells. Two studies incorporated C3 treatment and results are reported as the means \pm errors to the means.

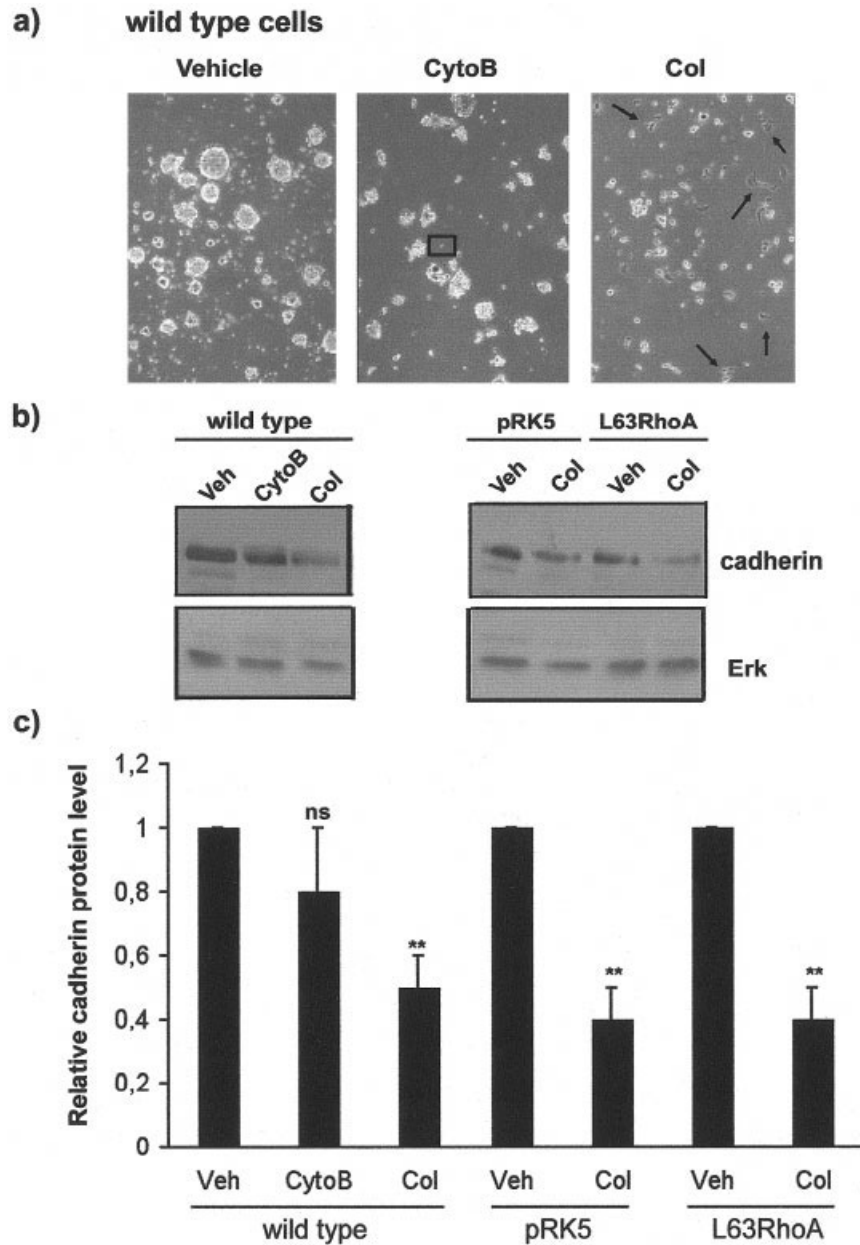


Figure 8 Microtubule disrupter reduces cadherin protein level during neurodetermination. Wild-type cells and cells transfected with myc tagged-L63RhoA cDNA or pRK5 empty plasmid (control) were treated for 24 h with vehicle (Veh; DMSO), 5 μ M cytochalasin B (CytoB), or 1 μ M colchicin (Col) starting at day 0 of the neurodifferentiation protocol. (a) Morphology of wild-type cells at end of treatment (100X). The square contains a single cell for size reference and arrows point to adhered cells. (b) Pan-cadherin Western blots, using Erk immunoreactivity as a control for gel loading. (c) Densitometric analysis of cadherin immunoblots. The symbols ns and ** respectively indicate no and highly significant difference with vehicle. Results are expressed as the means \pm SEM of five independent experiments.

level [Fig. 8(a–c), compare CytoB with Vehicle]. In contrast to cytochalasin B but similar to C3, colchicin, a disrupter of microtubules, significantly decreased cadherin level by 50% [Fig. 8(b,c)]. In addition,

colchicin did not support well the formation of aggregates and rather induced cell adhesion to bacteriological surfaces [Fig. 8(a)]. These results would indicate that the mechanism of C3 effect on cadherin has a

Table 2 Summary of Treatment Effects on Cadherin Protein Level and Cellular Adhesion in Neurally Differentiating Cell Aggregates

Treatment	Cadherin Protein Level	Cellular Adhesion		Culture Phenotype at Day 7
		Aggregate Cohesion	Adhesion to Bacteriological Surface	
C3 toxin*	↓	↓	↑	---
RhoA antisense	↓	↓	Nil	# Fibroblast-like cells ↑
ROCK inhibitor	↓	↓	↑	---
Actin poison	Nil	Nil or ↓	Nil	---
Microtubule poison	↓	↓	↑	---
Cdc42/Rac1	↓	↓	↑	---

* The reported C3 effects were abolished in cells expressing constitutively active RhoA. Nil, no effect; ↓, a slight decreasing effect; ↓, a significant decreasing effect; ↑, an increasing or induced effect; ---, not investigated.

microtubule-based component. While overexpression of active RhoA protected cells against the C3 effect on cadherin, this was not the case for colchicin. Indeed, colchicin decreased by half the level of cadherin in both L63RhoA-expressing cells and cells transfected with empty plasmid [Fig. 8(b,c)]. It is possible that RhoA acts on subpopulations of microtubules affected by colchicin. The morphology of L63RhoA-expressing cells after colchicin treatment resembled that of colchicin-treated wild-type cells (not shown).

DISCUSSION

Numerous studies have clearly demonstrated the involvement of RhoGTPases in neurite growth, axonal guidance, and synaptogenesis, all phenomena occurring in postmitotic steps of neurogenesis and in neuroregeneration (Lehmann et al., 1999; Luo, 2000; Sebök et al., 1999; Yuan et al., 2003). In the present study, we used the P19 cell model to address roles of Rho proteins in the early steps of neurogenesis. As summarized in Table 2, our results indicate that RhoA has an effect on cadherin protein level and cell-cell contacts (aggregate cohesion) during neuroinduction, with an influence on the efficiency of this process. The cellular effects are mediated by ROCK and seem to involve microtubules, pointing for the first time at the existence of a potential complex cross-talk between RhoA/ROCK, N-cadherin, and microtubules. As for RhoA inactivation, premature up-regulation of active Cdc42 decreased cadherin level and cell aggregation, suggesting that an adequate balance of RhoA and Cdc42 activity could be required in differentiating cells undergoing neurodetermination.

We previously showed that RhoA is up-regulated at the beginning of our neurodifferentiation protocol, that is, during aggregation, suggesting a role in cell

commitment to neuronal lineages mediated by cell-cell contacts (Laplante et al., 2001). The present work provides experimental evidence supporting this hypothesis, as inactivation of the RhoA/ROCK pathway with C3 toxin and kinase inhibitor decreased cell cohesion and cadherin level during neurodifferentiation (Figs. 1, 2, 6). In accordance with reduced cell-cell interaction, C3 toxin also down-regulated β - and α -catenin, which are necessary to the formation of adhesion complexes with cadherin (not shown). The effect on cadherin level occurred within a specific time window (Fig. 2), which corresponds to the switch of E- to N-cadherin known to trigger neurodifferentiation (Gao et al., 2001). N-cadherin level as well as cell cohesion appear to be critical to cell fate determination during morphogenic changes. Indeed, down-regulation of RhoA level by antisense strategy revealed that reduced N-cadherin level and cell cohesiveness increase the incidence of fibroblast-like cells relative to neurons upon RA treatment (Fig. 5). In agreement with this finding, Charrasse et al. (2002) observed that antibody- or low calcium-mediated blockade of N-cadherin-dependent contacts in mouse myoblast cultures impaired the pursuit of myogenesis.

Studies using epithelial and fibroblast-type cells expressing E-cadherin have shown that Rho activity regulates the recruitment of cadherin molecules and the formation of cadherin complexes at cell-cell contact sites without any impact on cadherin level (Braga et al., 1999, 2000; Braga, 2000; Engers et al., 2001; Hirase et al., 2001; Takaishi et al., 1997). In accordance with these observations, C3-induced Rho inactivation did not influence cadherin level in undifferentiated P19 cell populations expressing E-cadherin whether they were cultured as monolayers or aggregates (Fig. 2). Postmitotic P19 neurons expressing N-cadherin instead of E-cadherin responded like undifferentiated cells to C3 treatment (Fig. 4). These

results indicate that the temporary inactivation of Rho has no effect on cadherin level in cells having a stabilized phenotype. In contrast, C3 significantly decreased cadherin protein level during the switch from E- to N-cadherin that occurs at the beginning of the neurodifferentiation protocol.

C3 did not prevent occurrence of the E/N-cadherin switch and it did not abolish cadherin protein expression (Fig. 2) despite an almost complete inhibition of cell aggregation [Fig. 1(a), photo 6], suggesting a post-transcriptional action. The C3-induced decrease in cadherin level could be due to premature degradation of newly synthesized cadherin molecules. In an attempt to explore this possibility we found that cell exposure to lactacystin or chloroquine during C3 treatment did not inhibit C3-induced cadherin down-regulation (not shown), indicating that C3 did not stimulate the degradation of cadherin by the proteasome system or by lysosomes that are main intracellular routes of cadherin turnover (Tsukamoto and Nigram, 1999; Fujita et al., 2002). Another, yet unknown, degradation route (for example, extracellular proteases) could however exist. On the other hand, lower cadherin levels could result from slower translation rates probably associated with delayed transportation to the cell surface. Immaturity of newly assembled cytoskeleton elements could be implicated in the potentially reduced biological life/translation rate/transportation rate because the change from E- to N-cadherin conceivably commands a reorganization of the cytoskeleton (e.g., actin filaments and microtubules) for the establishment of new modes of cell interactions. The results of the introduction of constitutively active RhoA (L63RhoA) in P19 cells support the idea that RhoA has a stabilizing action on N-cadherin protein level rather than a direct effect on gene expression. Indeed, L63RhoA-transfected cells had not increased cadherin levels compared to mock-transfected cells, but had acquired the ability to resist C3-induced cadherin reduction [Fig. 3(c)].

Normally, E- and N-cadherin firmly engaged in cell-cell contacts are associated with actin cytoskeleton, the integrity of which is required to maintain cadherin at these plasma membrane sites (Krendel and Bonder, 1999; Mary et al., 2002; Menko et al., 2002). In various cell models, RhoA or ROCK inactivation was shown to disorganize the actin cytoskeleton (Ridley and Hall, 1992; Ridley et al., 1992; Maekawa et al., 1999). When we treated P19 aggregates with cytochalasin B during neuroinduction to disturb actin structure, we observed no significant cadherin down-regulation, whereas microtubule disruption with colchicin had a pronounced reducing effect (Fig. 8), revealing the importance of microtubule network in

the regulation of cadherin level. Although the underlying mechanism remains to be elucidated, this finding has relevance to the work of Mary et al. (2002), showing that N-cadherin shuttles between an intracellular (vesicular) and a plasma membrane pool in fibroblast and myoblast cultures, with the vesicular pool being tightly associated with, and transported by, the microtubule network. That P19 differentiating cells responded similarly to microtubule disruption and RhoA/ROCK inactivation strongly suggests that microtubules are a target of RhoA/ROCK action during neurodetermination. ROCK is well known for its action on actomyosin by phosphorylating myosin light chain, but other ROCK targets are being identified or proposed that belong to other cytoskeletal networks, such as intermediate filaments and microtubule associated-proteins (Amano et al., 2000). In fibroblasts, RhoA activation generates stable, detyrosinated microtubules but only of a subset of the microtubules (Cook et al., 1998). It is possible that RhoA action in P19 cells also targets a subpopulation of microtubules, explaining why overexpression of constitutively active RhoA prevented C3- but not colchicin-induced cadherin down-regulation (Figs. 3 and 8).

RhoA effect on cadherin level was observed before the important (20X) up-regulation that occurs from day 2 of aggregation (Laplante et al., 2001), indicating that RhoA has a role beyond neurodetermination. Cadherin engagement in cell-cell contacts was reported to activate Rho proteins (Charrasse et al., 2002; Kim et al., 2000; Noren et al., 2001), and we can conceivably think that Rho-initiated cadherin engagement could be further strengthened by a positive feedback circuit. Often RhoA and Cdc42/Rac1 were reported to have opposite effects and the present work provides another example of this behavior. In fact, overexpression of Cdc42/Rac1 had the same effects as RhoA inactivation on cell morphology and cadherin level in neurally differentiating cells (Fig. 7). Given the impact of RhoA inactivation in the P19 cell model, premature Cdc42 expression has the potential to affect neurodetermination efficiency. Several studies have revealed the existence of relationships between Cdc42/Rac1 and microtubules, militating in favor of the concept that RhoA and Cdc42/Rac1 cross-talking influences cadherin level via microtubule organization. Indeed, Cdc42/Rac1 can modulate the microtubule network by interacting with IQGAP1 and CLIP-170, Rac1 can bind to tubulin, and Cdc42 can interact with kinectin, an anchoring protein of microtubule kinesin motor (Best et al., 1996; Hotta et al., 1996; Fukata et al., 2002).

An intriguing finding of the present work is the

observation that impairment of cell aggregation by C3 toxin, ROCK inhibitor, and colchicin in neurally differentiating cells promoted cell adhesion to bacteriological-grade culture dishes, a polystyrene surface that does not normally allow adhesion [Fig. 1(a), photo 6; Fig. 6(a), photo 3; Fig. 8(a), Col]. Reasons for this unexpected adhesive behavior are unknown but integrins could have a role. Indeed, the formation of integrin-based focal complexes and focal adhesions in cell-matrix interaction involve Rho proteins in addition to actin (Fukata et al., 1999; Schmitz et al., 2000), and the control of integrin mobility in the plasma membrane was shown recently to implicate the participation of microtubules in Rho-independent as well as Rho-dependent mechanisms (Zhou et al., 2001). Considering these facts and knowing that a number of proteins that bridge integrins to the cytoskeleton are also involved in bridging cadherins to this structure (Bershadsky and Geiger, 1999), one can hypothesize that a decrease in cell-cell contacts in P19 cells would redirect some bridging proteins from cadherins towards integrins.

In conclusion, using the P19 cell model of neuronal differentiation, we demonstrated that RhoA is implicated in neurogenesis as early as during neurodetermination, where it influences cell-cell contact and cadherin level. These RhoA functions are ROCK-mediated and seem to involve the participation of microtubules. Advanced induction of Cdc42 had effects similar to RhoA inactivation, raising the importance of correct timing of RhoGTPases in neurodifferentiation. Further investigation is required to work out in detail the RhoA/ROCK mechanisms involved in cell adhesive properties during neurogenesis.

I.L. is the recipient of a FCAR studentship from the Gouvernement du Québec. We thank Dr Alan Hall (University College London, London, UK) for the gift of RhoA cDNAs, Dr Isabelle Royal (Université de Montréal, Montréal, Québec, Canada) for the gift of Cdc42 and Rac1 plasmids, and Dr. Borhane Annabi (Université du Québec à Montréal) for helpful criticism of the manuscript.

REFERENCES

- Adamson P, Paterson HF, Hall A. 1992. Intracellular localization of p21^{rho} proteins. *J Cell Biol* 119:617–627.
- Amano M, Fukata Y, Kaibuchi K. 2000. Regulation and functions of Rho-associated kinase. *Exp Cell Res* 261:44–51.
- Arthur WT, Noren NK, Burrige K. 2002. Regulation of Rho family GTPases by cell-cell and cell-matrix adhesion. *Biol Res* 35:239–246.
- Barth H, Olenik C, Sehr P, Schmidt G, Aktories K, Meyer DK. 1999. Neosynthesis and activation of Rho by Escherichia coli cytotoxic necrotizing factor (CNF1) reverse cytopathic effects of ADP-ribosylated Rho. *J Biol Chem* 274:27407–27414.
- Beltman J, Erickson JR, Martin GA, Lyons JF, Cook SJ. 1999. C3 toxin activates the stress signaling pathways, JNK and p38, but antagonizes the activation of AP-1 in rat-1 cells. *J Biol Chem* 274:3772–3780.
- Bershadsky A, Geiger B. 1999. Cytoskeleton-associated anchor and signal transduction proteins. In: Kreis T, Vale R, editors. *Guidebook to the extracellular matrix, anchor, and adhesion proteins*. New York: Oxford University Press, p 3–11.
- Best A, Ahmed S, Kozma R, Lim L. 1996. The Ras-related GTPase Rac1 binds tubulin. *J Biol Chem* 271:3756–3762.
- Bito H, Furuyashiki T, Ishihara H, Shibasaki Y, Ohashi K, Mizuno K, Maekawa M, Ishizaki T, Narumiya S. 2000. A critical role for a Rho-associated kinase, p160ROCK, in determining axon outgrowth in mammalian CNS neurons. *Neuron* 26:431–441.
- Braga V. 2000. Epithelial cell shape: cadherins and small GTPases. *Exp Cell Res* 261:83–90.
- Braga V. 2002. Cell-cell adhesion and signalling. *Curr Opin Cell Biol* 14:546–556.
- Braga VMM, Betson M, Xiaodong L, Lamarche-Vane N. 2000. Activation of the small GTPase Rac is sufficient to disrupt cadherin-dependent cell-cell adhesion in normal keratinocytes. *Mol Biol Cell* 11:3703–3721.
- Braga VMM, Del Maschio A, Marchesky L, Dejana E. 1999. Regulation of cadherin function by Rho and Rac: Modulation by junction maturation and cellular context. *Mol Biol Cell* 10:9–22.
- Brewer GJ. 1995. Serum-free B27/neurobasal medium supports differentiated growth of neurons from the striatum, substantia nigra, septum, cerebral cortex, cerebellum, and dentate gyrus. *J Neurosci Res* 42:674–683.
- Cadet N, Paquin J. 2000. Conversion and storage of somatostatin are established before response to secretagogue stimuli in P19 neurons. *Brain Res Dev Brain Res* 120:211–221.
- Charrasse S, Meriane M, Comunale F, Blangy A, Gauthier-Rouviere C. 2002. N-cadherin-dependent cell-cell contact regulates Rho GTPases and β -catenin localization in mouse C2C12 myoblasts. *J Cell Biol* 158:953–965.
- Chung CT, Niemela SL, Miller RH. 1989. One-step preparation of competent Escherichia coli: transformation and storage of bacterial cells in the same solution. *Proc Natl Acad Sci USA* 86:2172–2175.
- Clayton L, Hall A, Johnson MH. 1999. A role for Rho-like GTPases in the polarization of mouse eight-cell blastomeres. *Dev Biol* 205:322–331.
- Cook TA, Nagasaki T, Gundersen GG. 1998. Rho guanosine triphosphatase mediates the selective stabilization of microtubules induced by lysophosphatidic acid. *J Cell Biol* 141:175–185.
- Denhardt DT. 1996. Signal-transducing protein phosphorylation cascades mediated by Ras/Rho proteins in the

- mammalian cell : the potential for multiplex signalling. *Biochem J* 318:729–747.
- Engers R, Springer E, Michiels F, Collard JO, Gabbert HE. 2001. Rac affects invasion of human renal cell carcinomas by upregulating TIMP-1 and TIMP-2. *J Biol Cell* 276:41889–41897.
- Fujita Y, Krause G, Scheffner M, Zechner D, Leddy HE, Behrens J, Sommer T, Birchmeier W. 2002. Hakai, a c-Cbl-like protein, ubiquitinates and induces endocytosis of E-cadherin complex. *Nature Cell Biol* 4:222–231.
- Fukata M, Kaibuchi K. 2001. Rho-family GTPases in cadherin-mediated cell-cell adhesion. *Nature Rev* 2:887–897.
- Fukata M, Nakagawa M, Kudora S, Kaibuchi K. 1999. Cell adhesion and Rho small GTPases. *J Cell Sci* 112:4491–4500.
- Fukata M, Watanabe T, Noritake J, Nakagawa M, Yamaga M, Kuroda S, Matsuura Y, Iwamatsu A, Perez F, Kaibuchi K. 2002. Rac1 and Cdc42 capture microtubules through IQGAP1 and CLIP-170. *Cell* 109:873–885.
- Gao X, Bian W, Yang J, Tang K, Kitani H, Atsumi T, Jing N. 2001. A role of N-cadherin in neuronal differentiation of embryonic carcinoma P19 cells. *Biochem Biophys Res Commun* 284:1098–1103.
- Gingras D, Lamy S, Beliveau R. 2000. Tyrosine phosphorylation of the vascular endothelial- growth-factor receptor-2 (VEGFR-2) is modulated by Rho proteins. *Biochem J* 348 (Pt 2):273–280.
- Hall A. 1998. Rho GTPases and actin cytoskeleton. *Science* 279:509–514.
- Hatten ME. 1999. Central nervous system neuronal migration. *Ann Rev Neurosci* 22:238–252.
- Hirase T, Kawashima S, Wong EY, Ueyama T, Rikitake Y, Tsukita S, Yokoyama M, Staddon JM. 2001. Regulation of tight junction permeability and occludin phosphorylation by RhoA- p160ROCK-dependent and -independent pathway. *J Biol Chem* 276:10423–10431.
- Hirose M, Ishizaki T, Watanabe N, Uehata M, Kranenburg O, Moolenaar WH, Matsumura F, Maekawa M, Bito H, Narumiya S. 1998. Molecular dissection of the Rho-associated protein kinase (p160ROCK)-regulated neurite remodeling in neuroblastoma N1E 115 cells. *J Cell Biol* 141:1625–1636.
- Hotta K, Tanaka K, Mino A, Kohno H, Takai Y. 1996. Interaction of the Rho family small G proteins with kinectin, an anchoring protein of kinesin motor. *Biochem Biophys Res Commun* 225:69–74.
- Jalink K, van Corven EJ, Hengelveld T, Morii N, Narumiya S, Moolenaar WH. 1994. Inhibition of lysophosphatidate- and thrombin-induced neurite retraction and neuronal cell rounding by ADP ribosylation of the small GTP-binding protein Rho. *J Cell Biol* 126:801–810.
- Jeannotte R, Paquin J, Petit-Turcotte C, Day R. 1997. Convertase PC2 and the neuroendocrine polypeptide 7B2 are co-induced and processed during neuronal differentiation of P19 embryonal carcinoma cells. *DNA Cell Biol* 16: 1175–1187.
- Kaibuchi K, Kuroda S, Fukata M, Nakagawa M. 1999. Regulation of cadherin-mediated cell-cell adhesion by the Rho family GTPases. *Curr Opin Cell Biol* 11:591–596.
- Kim SH, Li Z, Sacks D. 2000. E-cadherin-mediated cell-cell attachment activates Cdc42. *J Biol Chem* 275:36999–37005.
- Kjøller L, Hall A. 1999. Signaling to Rho GTPases. *Exp Cell Res* 253:166–179.
- Krendel MF, Bonder EM. 1999. Analysis of actin filament bundle dynamics during contact formation in live epithelial cells. *Cell Motil Cytoskeleton* 43:296–309.
- Laemmli UK. 1970. Cleavage of structural proteins during the head of bacteriophage T4. *Nature* 227:680–685.
- Laplante I, Paquin J, Beliveau R. 2001. RhoB expression is induced after transient upregulation of RhoA and Cdc42 during neuronal differentiation and influenced by culture substratum and microtubule integrity. *Brain Res Dev Brain Res* 129:157–168.
- Lehmann M, Fournier A, Selles-Navarro I, Dergham P, Sebok A, Leclerc N, Tigyi G, McKerracher L. 1999. Inactivation of Rho signalling pathway promotes CNS axon regeneration. *J Neurosci* 19:7537–7547.
- Liu BP, Chrzanowska-Wodnicka M, Burrridge K. 1998. Microtubule depolymerization induces stress fibers, focal adhesion, and DNA synthesis via the GTP-binding protein Rho. *Cell Adhes Commun* 5:249–255.
- Luo L. 2000. Rho GTPases in neuronal morphogenesis. *Nature Rev* 1:173–180.
- Maekawa M, Ishizaki T, Boku S, Watanabe N, Fujita A, Iwamatsu A, Obinata T, Ohashi K, Mizuno K, Narumiya S. 1999. Signaling from Rho to the actin cytoskeleton through protein kinases ROCK and LIM-kinase. *Science* 285:895–898.
- Mary S, Charrasse S, Meriane M, Comunale F, Trao P, Blangy A, Gauthier-Rouviere C. 2002. Biogenesis of N-cadherin-dependent cell-cell contacts in living fibroblasts is a microtubule-dependent kinesin-driven mechanism. *Mol Biol Cell* 13:285–301.
- McBurney MW. 1993. P19 embryonal carcinoma cells. *Int J Dev Biol* 37:135–140.
- Menko AS, Zhang L, Schiano F, Kreidberg JA, Kukuruzinska MA. 2002. Regulation of cadherin junctions during mouse submandibular gland development. *Dev Dyn* 224: 321–333.
- Natale DR, Watson AJ. 2002. Rac-1 and IQGAP are potential regulators of E-cadherin-catenin interactions during murine preimplantation development. *Gene Expr Patterns* 2:17–22.
- Nikolic M. 2002. The role of Rho GTPases and associated kinases in regulating neurite outgrowth. *Int J Biochem Cell Biol* 34:731–745.
- Noren NK, Arthur WT, Burrridge K. 2003. Cadherin engagement inhibits RhoA via p190RhoGAP. *J Biol Chem* 278:13615–13618.
- Noren NK, Niessen CM, Gumbiner BM, Burrridge K. 2001. Cadherin engagement regulates Rho family GTPases. *J Biol Chem* 276:33305–33308.
- Paquin J, Danalache B, Jankowski M, McCann SM, Gutkowska J. 2002. Oxytocin induces differentiation of P19

- embryonic stem cells to cardiomyocytes. *Proc Nat Acad Sci USA* 99:9550–9555.
- Redies C. 2000. Cadherins in the central nervous system. *Prog Neurobiol* 61:611–648.
- Ridley AJ. 1997. The GTP-binding protein Rho. *Int J Biochem Cell Biol* 29:1225–1229.
- Ridley AJ, Hall A. 1992. The small GTP-binding protein rho regulate the assembly of focal adhesions and actin stress fibers in response to growth factors. *Cell* 70:389–399.
- Ridley AJ, Paterson HF, Johnston CL, Diekmann D, Hall A. 1992. The small GTP-binding protein rac regulates growth factor-induced membrane ruffling. *Cell* 70:401–410.
- Royal I, Lamarche-Vane N, Lamorte L, Kaibuchi K, Park M. 2000. Activation of Cdc42, Rac, PAK, and Rho-kinase in response to hepatocyte growth factor differentially regulates epithelial cell colony spreading and dissociation. *Mol Biol Cell* 11:1709–1725.
- Rudnicki MA, McBurney MW. 1987. Cell culture methods and induction of differentiation of embryonal carcinoma cell lines. In: Robertson EJ editor. *Teratocarcinomas and Embryonic Stem Cells: A Practical Approach*. Oxford: IRL Press, p 19–49.
- Schmitz AAP, Govek EE, Böttner B, Van Aelst L. 2000. Rho GTPases : signaling, migration, and invasion. *Exp Cell Res* 261:1–12.
- Seböck A, Nusse N, Debreceni B, Guo Z, Santos MF, Szberenyi J, Tigyi G. 1999. Different roles for RhoA during neurite initiation, elongation, and regeneration in PC12 cells. *J Neurochem* 73:949–960.
- Sugihara K, Nakatsuji N, Nakamura K, Nakao N, Hashimoto R, Otani H, Sakagami H, Kondo H, Nozawa S, Aiba A, et al. 1998. Rac1 is required for the formation of three germ layers during gastrulation. *Oncogene* 17:3427–3433.
- Takai Y, Sasaki T, Matozaki T. 2001. Small GTP-binding proteins. *Physiol Rev* 81:153–208.
- Takaishi K, Sasaki T, Kotani H, Nishioka H, Takai Y. 1997. Regulation of cell-cell adhesion by Rac and Rho small G proteins in MDCK cells. *J Cell Biol* 10:1047–1059.
- Tsukamoto T, Nigram SK. 1999. Cell-cell dissociation upon epithelial cell scattering requires a step mediated by proteasome. *J Biol Chem* 274:24579–24584.
- Wittmann T, Waterman-Storer CM. 2001. Cell motility: can Rho GTPases and microtubules point the way? *J Cell Sci* 114:3795–3803.
- Yagi T, Takeichi M. 2000. Cadherin superfamily genes : functions, genomic organization, and neurologic diversity. *Genes Dev* 14:1169–1180.
- Yuan X, Jin M, Xu X, Song Y, Wu C, Poo M, Duan S. 2003. Signalling and cross-talk of RhoGTPases in mediating axon guidance. *Nature Cell Biol* 5:1–8.
- Zhou X, Li J, Kucik DF. 2001. The microtubule cytoskeleton participates in control of β_2 integrin avidity. *J Biol Chem* 276:44762–44769.